The Eurasia Proceedings of Science, Technology, Engineering & Mathematics (EPSTEM)
ISSN: 2602-3199

The Eurasia Proceedings of Science, Technology, Engineering & Mathematics (EPSTEM), 2024

Volume 28, Pages 352-359

ICBASET 2024: International Conference on Basic Sciences, Engineering and Technology

Analysis of a High-Pressure Reciprocating Compressor Piston's 2D Simulation Utilizing Computational Fluid Dynamics

Furkan Turgut
Logos Kimya Teknolojileri Ltd. Şti.

Ahmet Berkay Simsek
Middle East Technical University

Necip Berker Uner
Middle East Technical University

Bariş Erdogan
Logos Kimya Teknolojileri Ltd. Sti.

Abstract: Reciprocating compressors represent the most renowned and extensively utilized compressors within the positive displacement category. A compressor that takes input gas at pressures above atmospheric and delivers it very high pressures (> 100 bar) is specifically called a booster pump. These pumps commonly consist of two or more piston-cylinder units in series, connected through check valves that determine the final delivery pressure, and they are instrumental in a range of applications centered around the storage and delivery of gases and fuels. Despite the availability of various booster pumps in the global market, literature offers limited insights into their design specifics. The design intricacies of a booster pump, tailored to operate at specified output pressure and mass flow rate, are contingent upon the interplay of coupled flow dynamics and heat transfer phenomena within the system. These phenomena include fluid flow dynamics through check valves, heat transfer across cylinder walls, and mechanical properties of pump materials, alongside cyclic operational parameters. To address this gap, we have embarked on an experimental-computational investigation aimed at elucidating the transport processes occurring in a single-cylinder booster pump. This work focuses on computational investigations concerning gas compression and the actuation of check valves in a single-cylinder reciprocating booster. Momentum and energy conservation equations were solved on a dynamic mesh platform through Ansys Fluent. Adiabatic conditions were employed, and the numerical solver was partially validated by comparison with thermodynamic theory for simulations conducted in a closed adiabatic cylinder. Calculations were then extended for an open cylinder with inlet and outlet check valves. Simulations indicate that forced cooling plays an important role for the longevity of sealing parts.

Keywords: Compressors, Fluid dynamics, ANSYS Fluent, CFD

Introduction

Compressors display a rich collection of gas dynamics, where fluid flow, thermodynamics and heat transfer become coupled to each other and consequently determine the specifications of the device. The goal is to increase the pressure of a gas in a semi-continuous manner, which results in heating of the gas. The extent of heating is directly proportional to the increase in pressure and the rate of cooling in the compressor.

High temperature and pressure presents challenges in the design of compressors, especially in terms of materials selection. Therefore, fundamental compressor elements harbor specific design-limiting operational conditions.

In instances where limitations are encountered, the execution of work often necessitates an increase in the number of compression processes, a strategy termed multi-staging. This involves employing a core machine element designed to operate sequentially with other components of the machinery. (Bloch et al., 1996). Although the nature of these limitations' changes with respect to the compressor type, the major design parameters that are common to all compressors are listed graphically in Figure 1 below.

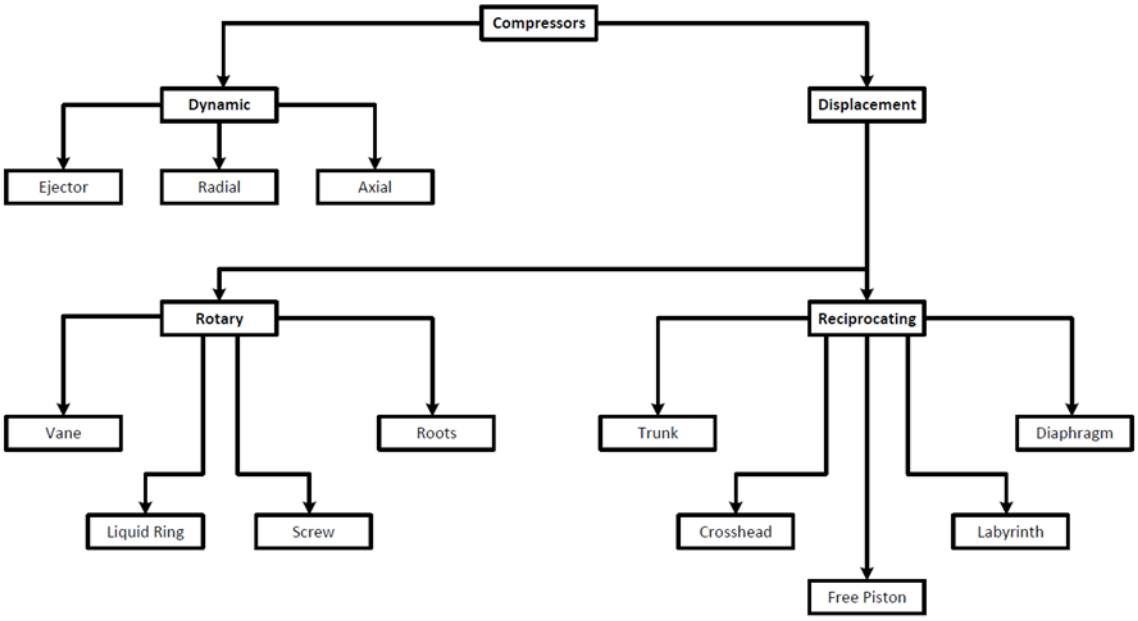

Figure 1. Primary types of compressors.

The primary types of compressors shown in Figure 1 are summarized below. Cam, diaphragm, and diffusion compressors are omitted due to their specialized applications and relatively compact sizes.

Dynamic Compressors: These rotary continuous-flow machines utilize a rapidly rotating element to accelerate gas, converting velocity head into pressure. This process occurs both in the rotating element and stationary diffusers or blades.

Centrifugal Compressors: Dynamic machines where one or more rotating impellers, typically shrouded on the sides, accelerate the gas. The main gas flow is radial.

Axial Compressors: Dynamic machines employing the bladed rotor's action for gas acceleration. Main gas flow is axial.

Positive Displacement Units: Positive displacement units confine successive gas volumes within a closed space and elevate them to a higher pressure.

Rotary Positive Displacement Compressors: These machines achieve compression and displacement through the positive action of rotating elements.

Sliding Vane Compressors: A subset of rotary positive displacement machines, sliding vane compressors feature axial vanes sliding radially in a rotor eccentrically mounted in a cylindrical casing. Gas trapped between vanes undergoes compression and displacement. (Duprez et al., 2007)

Liquid Piston Compressors: In these rotary positive displacement machines, water or another liquid serves as the piston to compress and displace the handled gas.

Two-Impeller Straight-Lobe Compressors: Rotary positive displacement machines with two straight mating lobed impellers that trap and convey gas from intake to discharge. Internal compression is absent.

Helical or Spiral Lobe Compressors: This category comprises rotary positive displacement machines where two intermeshing rotors, each with a helical form, compress and displace the gas.

Mixed Flow Compressors: Dynamic machines with an impeller form that combines characteristics of both centrifugal and axial types.

This classification summarized above sheds light on the diverse array of compressors, each tailored to specific applications and operational principles. (Roskosch et al., 2017) When considering compressor classifications, the reciprocating crosshead compressor is the model we aim to design for elevating a low-pressure gas to a high pressure. Its widespread preference in the market and our mechanical design expertise in this subject have been influential factors in selecting this compressor model.

In this study, the objective is to design a single-piston, high-pressure reciprocating crosshead compressor, which may also be referred to as a booster pump. In addition to the mechanical analyses currently being conducted, our group concentrates on investigating the flow system. This paper is a report of preliminary calculations done via computational fluid dynamics (CFD). Using the Ansys Fluent, dynamic simulations of closed piston compression were done, and calculations were verified against adiabatic compression calculations. Simulations were then extended to the case with flow, allowing adiabatic temperatures to be estimated.

Method

In the calculations presented below, fluid mechanics and heat transfer are interlinked, and the computational domain undergoes deformation throughout the compression process. In models where the computational domain changes during the simulation, the mesh structure also needs to evolve over time. It is crucial to test the accuracy of the results produced by such dynamic models with existing theory or experiments. Fortunately, thermodynamics offer a very simple description of reversible and adiabatic process, therefore Fluent simulations were initially focused on adiabatic compression in a closed cylinder.

Adiabatic compression is an isentropic process when reversible. Assuming a constant heat capacity ratio $\gamma = C_p/C_v$ for an ideal gas during compression, the following equations are valid for pressure and temperature in the cylinder, where subscript 1 denotes the state with a fully withdrawn piston and subscript 2 denotes a fully compressed chamber.

$$P_2 = P_1\left(\frac{V_1}{V_2}\right)^{\gamma}$$

$$T_2 = T_1\left(\frac{V_1}{V_2}\right)^{\gamma-1}$$

By solving the momentum and energy conservation equations in Fluent for compression of argon, and assuming argon to be an ideal gas with constant physical parameters (e.g., C_p, μ, etc.), the calculated values of P_2 and T_2 in adiabatic simulations are expected to equal to thermodynamic values provided above. The primary reason for this expectation is that the generation of entropy caused by piston friction is not included in the simulation. Therefore, a major source of irreversibility is removed, and thanks to slow compression speeds usually employed in booster pumps, the gas is expected to be at conditions close to thermodynamic equilibrium.

Table 1. Parameters used in ANSYS Fluent calculations.

Parameter	**Value**	**Unit**
Shaft Speed	72	rpm
Crank Diameter	19	mm
Crank Period	360	degree
Rod Lenght	70	mm
Cylinder Diameter	19.05	mm
Stroke	39	mm
Starting Temperature	300	K
Starting Pressure	40	bar

Compression calculations were performed for the given piston parameters to achieve a compression ratio, V_1/V_2, of 39. The calculations were conducted considering turbulent flow, employing both 2D and 3D models. The 3D

model results presented below are of preliminary status and will be further developed to encompass the entire process in the future. Parameters used in the simulations are given in Table 1.

Results and Discussion

For the closed cylinder, results for pressure and temperature are presented in the two figures below. Deviations in the trends of pressure and temperature during compression as shown in Figure 2, where the compression volume is reduced, indicate the need for the development of a better moving mesh infrastructure in both 2D and 3D models. The 2D model showed more consistent results with isentropic calculations compared to the 3D model. This is primarily attributed to the relatively homogeneous mesh structure that can be created in the 2D geometry. It is believed that the cylinder compression rate is sufficiently slow, thus the calculations follow the adiabatic curves at small compression ratios. The inability to approach the thermodynamic results indicated deficiencies in numerical calculations and mesh infrastructure, especially when the compression ratio became larger than 5.

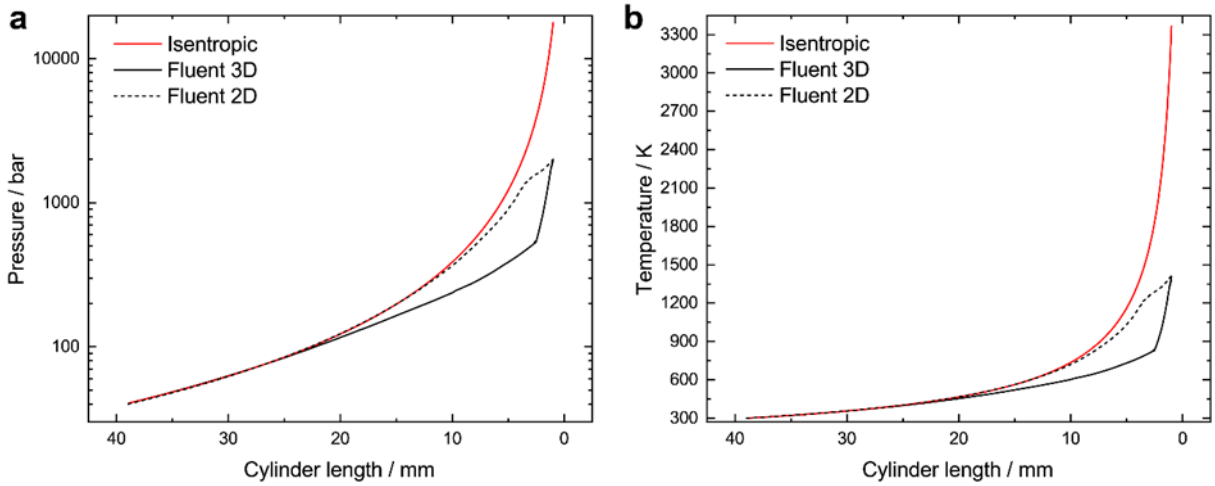

Figure 2. Preliminary calculations of compression within a closed and adiabatic cylinder for validation purposes. (a) pressure, (b) temperature. Both the 2D and 3D calculations suffered from insufficient meshing detail (see below).

The impact of mesh density on the results was investigated in the 2D model. The calculations revealed that increasing mesh density led to results approaching thermodynamic expectations. Achieving a close match to isentropic results was facilitated by a higher resolution in resolving the wall layer in the turbulence model, resolving pressure in tandem with velocity, and employing higher-order formulas in the finite volume discretization process. The outcomes of these calculations are presented below in Figure 3.

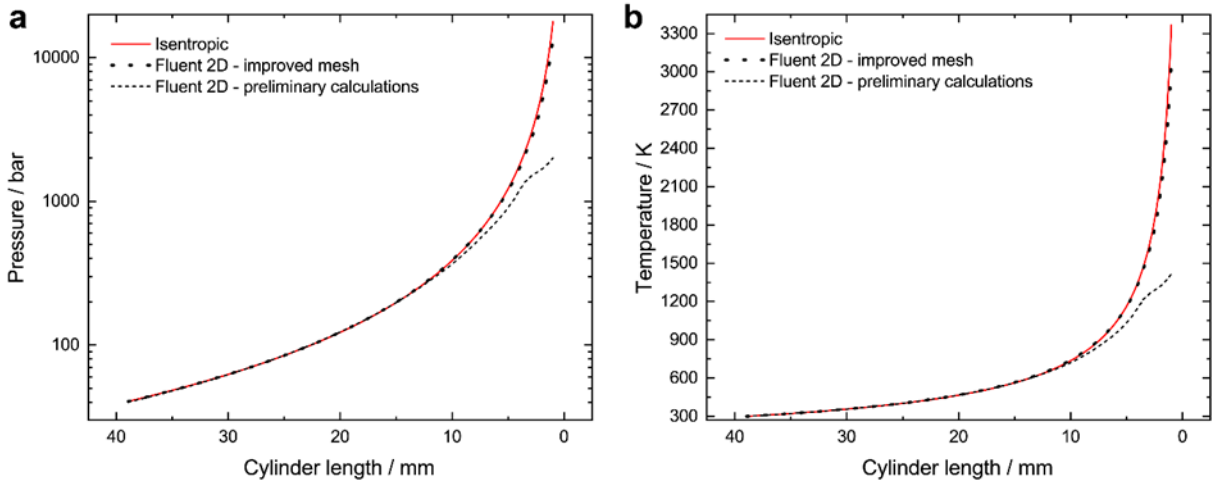

Figure 3. Two-dimensional calculations conducted for validation purposes within a closed and adiabatic cylinder.

The pressure and temperature within the closed and adiabatic cylinder during compression are depicted in Figure 3a and 3b respectively. Advanced calculations showcase the improvements in both the calculation and mesh infrastructure. Thus, a numerical calculation infrastructure that can either be transferred to a 3D model, used with inlet and outlet check valves, or with a second cylinder was established.

Due to the superior performance of 2D results compared to 3D, further model improvements was implemented on the 2D infrastructure. Utilizing the solver parameters that validated the thermodynamic results, the geometry of the piston was upgraded and an entry and exit region for argon was added. Gas flow characteristics was determined by check valves located at the inlet and outlet of the cylinder. The updated geometry is illustrated in the figure below.

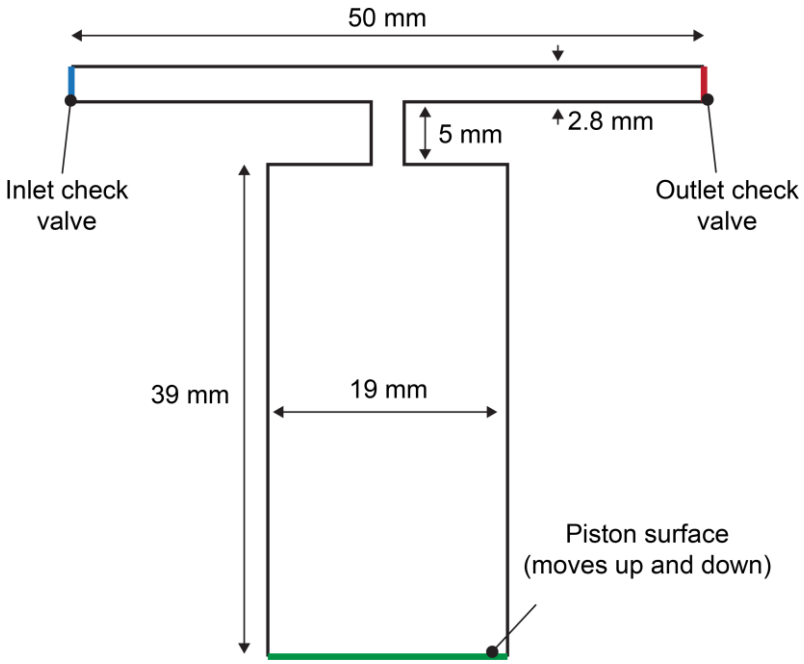

Figure 4. Updated cylinder geometry. The surfaces on the right and left sides of the structure correspond to the inlet and outlet of the check valve, respectively.

Gas flow through the check valves was added to the simulation by writing subroutines in Fluent (User Defined Function: UDF). The UDF algorithm dynamically integrates gas inlet or outlet calculations with cylinder movement and allows flow when the pressure difference across a check valve is reached. When the cracking pressure (1 bar) is exceeded, flow becomes unidirectional through the valve, whereas the valve closes when the differential pressure drops below the cracking pressure. The flow when the check valves are open is expressed by a general conductance equation:

$$\dot{m} = K \rho A_c \left(P_u - P_d \right)$$

Here, K denotes the flow conductance, and it was calculated assuming laminar flow in the cylindrical pipe-like flow geometry in the check valves. P_u and P_d represent the pressures upstream and downstream of the check valve, respectively, while ρ symbolizes the density of the argon gas upstream of the check valve, and A_c represents the cross-sectional area for flow through the check valve. K is calculated using the Hagen-Poiseuille equation, and A_c is initially calculated assuming the entire internal geometry of the check valve is a cylindrical pipe, then it was adjusted as a regression parameter based on the previous measurements conducted on the cylinder (LOGOS Kimya Teknolojileri Ltd. Sti., 2023.)

Computational results obtained for a full compression cycle is given in Figure 5, on which the compression of argon gas by the piston (1), the opening of the outlet valve (2), the retraction of the piston (3), and finally the opening of the inlet valve (4) are shown. It was observed that the volume change in both the pressure downstream of the inlet valve and the pressure upstream of the outlet valve is consistent and realistic, considering experiments previously conducted. It was observed that there was little to no pressure distribution inside the cylinder. In accordance with this result, pressures given in Figure 5 can be accepted to be valid for the entire geometry shown in Figure 4.

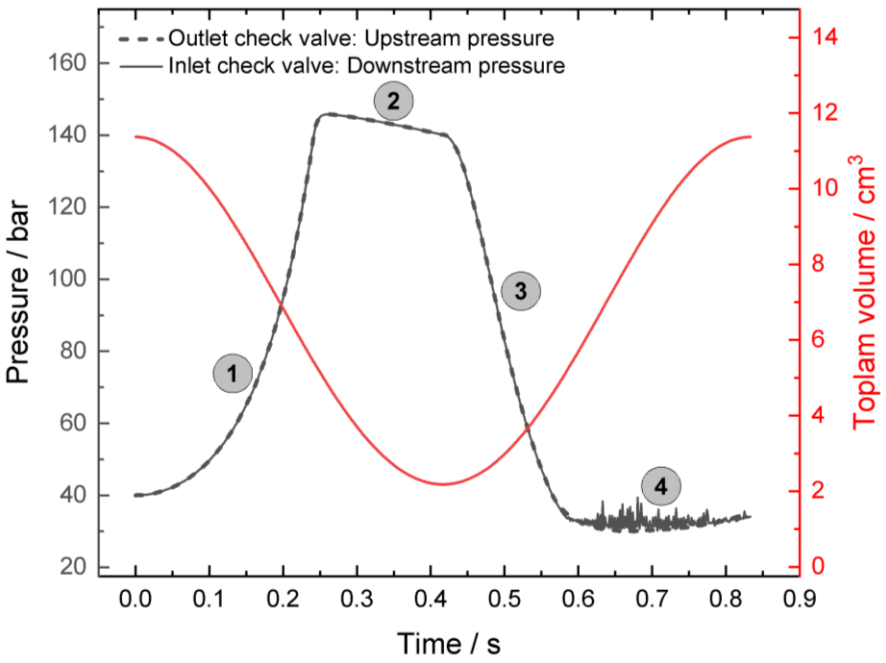

Figure 5. Pressure and volume versus time across the first compression cycle.

The initial pressure for this and the following two figures is 40 bars, the outlet pressure is 139 bars, and the cracking pressures of the check valves are 1 bar. In the calculations, the total volume of the tee pipes and the barrel is 11.4 cm³. The numbered stages are indicated in the text.

The fluctuation in inlet pressure following the opening of the inlet check valve is interpreted as numerical instability. In future calculations, this instability is aimed to be eliminated by taking the downstream pressure, P_d, in the conductance equation from a plane further away from the inlet surface instead of extracting it directly at the inlet surface. Since there is no pressure distribution inside the cylinder, this solution is expected to be valid. Figure 6 shows the mass flow rate during this cycle and similar fluctuations arising from the same reason are also observed. The inlet mass flow rate and outlet are noticeably different, which indicates that further cycles are required to reach a periodic steady-state.

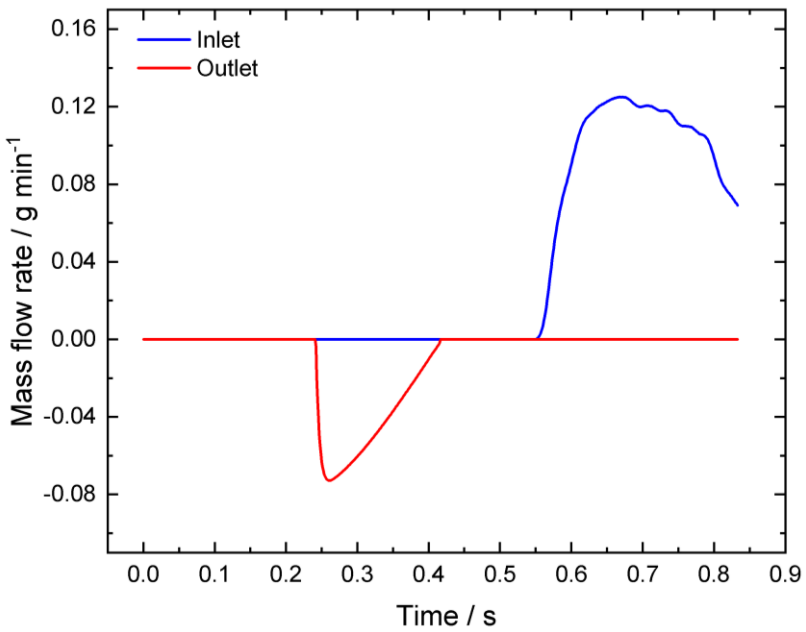

Figure 6. Mass flow versus time across the first compression cycle. During the period when the outlet valve is open (174 ms), the total amount of argon flowing is calculated as 0.12 mg. This corresponds to a rate of 8.67 g of argon per minute.

The temperature inside the barrel follows a similar trend to the pressure data except for the period that involves filling the cylinder with gas (Figure 7). Due to the adiabatic nature of the calculations and the assumption of an inlet gas temperature of 25°C as the boundary condition, cooling is observed nearby the gas inlet due to adiabatic expansion. Furthermore, temperatures exceeding 200 °C are observed due to adiabatic conditions. This observation indicates that cooling the cylinder will be important as most sealing materials, e.g. PTFE, have continuous service temperatures of approximately 200 °C.

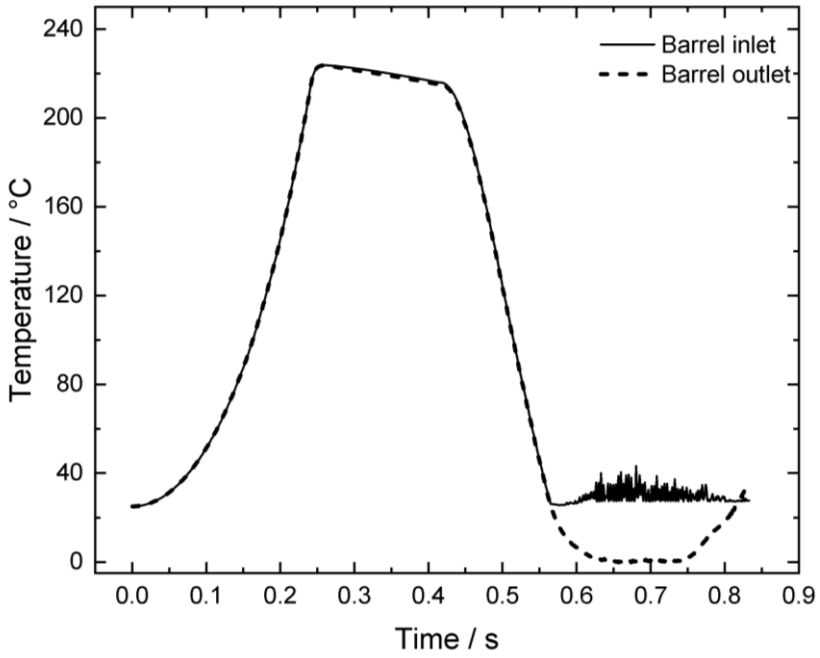

Figure 7. Temperature versus across the first compression cycle.

P-V diagram was seen to be similar to that of a reversible and adiabatic piston-cylinder (Cengel et al., 2011), except for some slight curvature at the horizontal sections, which are deviations from isobaric conditions that stem from the fluid dynamics associated with check valves (Figure 8). The gap at bottom left corner is an indication that periodic steady-state conditions have not been reached at the end of a single cycle, and more cycles are required.

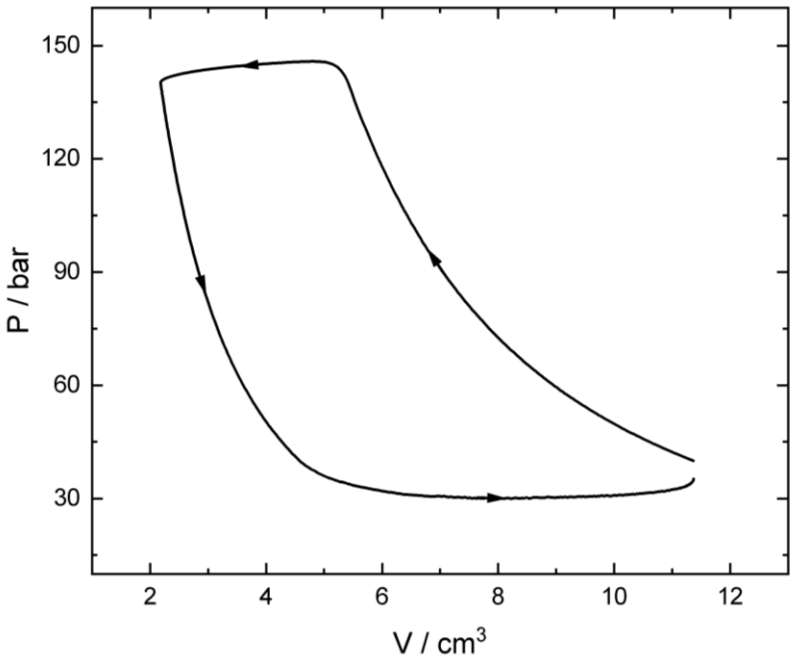

Figure 8. P-V diagram for the first compression cycle.

Conclusion

The studies indicate successful calculation of flow and temperature values for the operational state of a reciprocating compressor piston using Ansys Fluent software for 2D modeling. Adiabatic pressure and temperature values were observed to match theoretical values in a 2D piston model, with mesh parameters playing a significant role in achieving the desired accuracy. Subsequently, a model geometry with macroscopically modeled check valve was created with inlet and outlet connections similar to those in an actual booster pump. Here again, the obtained results were observed to resemble the actual piston compressor data. UDFs were used in the design of the check valves, which semi-empirically resulted in realistic trends in pressure during infilling and exhaust. Subsequent efforts will aim to implement heat losses and more fundamental check valve flow dynamics.

Scientific Ethics Declaration

The authors declare that the scientific ethical and legal responsibility of this article published in EPSTEM journal belongs to the authors.

Acknowledgements or Notes

* This article was presented as an oral presentation at the International Conference on Basic Sciences, Engineering and Technology (www.icbaset.net) held in Alanya/Turkey on May 02-05, 2024.

References

Bloch, H. P., & Hoefner, J. J. (1996). *Reciprocating compressors: Operation and maintenance.* Elsevier.

Cengel, Y. A., Boles, M. A., & KanoGlu, M. (2011). *Thermodynamics: an engineering approach (Vol.* 5, p. 445.) New York, NY: McGraw-hill.

Duprez, M. E., Dumont, E., & Frère, M. (2007). Modelling of reciprocating and scroll compressors. *International Journal of Refrigeration, 30*(5), 873-886.

Roskosch, D., Venzik, V., & Atakan, B. (2017). Thermodynamic model for reciprocating compressors with the focus on fluid dependent efficiencies. *International Journal of Refrigeration, 84*, 104-116.

Schultheis, S., Lickteig, C., & Parchewsky, R. (2011). Reciprocating compressor condition monitoring. In *Middle East Turbomachinery Symposia*. Texas A&M University,Turbomachinery Laboratories.

Author Information

Furkan Turgut
Logos Kimya Teknolojileri Ltd.Sti.
Gul Sanayi Sitesi, 1151. Sokak, No. 89,
Ostim / Ankara/Türkiye
Contact e-mail: *furkan@logoskimya.com*

Ahmet Berkay Simsek
Middle East Technical University
CZ-11 Dumlupınar Bulv. No.1 Cankaya 06800
Ankara/Türkiye

Necip Berker Uner
Middle East Technical University
D-110 Dumlupınar Bulv. No.1 Cankaya 06800
Ankara/Türkiye

Barıs Erdogan
Logos Kimya Teknolojileri Ltd. Sti.
Gül Sanayi Sitesi, 1151. Sokak, No. 89,
Ostim / Ankara/Türkiye

To cite this article:

Turgut, F., Simsek, A. B., Uner, N. B. & Erdogan, B. (2024). Analysis of a high-pressure reciprocating compressor piston's 2D simulation utilizing computational fluid dynamics. *The Eurasia Proceedings of Science, Technology, Engineering & Mathematics (EPSTEM), 28*, 352-359.